

Chapter 5

Recent Progress in Nanodielectric Composites and Their Applications



Joshi Harsh Nitinkumar, Navyasree Reghu, P. K. Akhilesh, Alexandru Vlad, Meera Balachandran, and Prasanth Raghavan

Abstract With the tremendous growth in electrical gadgets and electrification in recent years, there is an urgent need to utilise green/renewable energy and improve energy efficiency, energy conversion systems, and energy storage density. In the future, development in electrical power technologies will be aligned in the direction of higher power and frequency, wider bandwidth, faster speed, smaller form factor, higher temperature rating, lower cost, greater flexibility, and scalability. In this context, polymer nanocomposite dielectrics, also known as nanodielectrics, have garnered considerable scientific interest. Polymer nanodielectric combines the advantages of high dielectric constant nanofillers with high dielectric breakdown strength polymer matrix and offers the flexibility of engineering materials and structures to obtain desired and unique properties. This chapter discusses current developments in nanodielectric composites for energy storage applications with an emphasis on fundamental material concerns for two different types of polymer nanodielectrics: composites of polymer and ceramic and conductive nanoparticles. The role of tuneable nonlinear nanodielectrics in energy storage and harvesting is also discussed. The chapter highlights the applications, opportunities, and challenges associated with future developments in nanodielectrics.

J. H. Nitinkumar · N. Reghu · M. Balachandran (✉)

Department of Chemical Engineering and Materials Science, Amrita School of Engineering, Amrita Vishwa Vidyapeetham, Coimbatore 641112, India

e-mail: b_meera@cb.amrita.edu

Centre of Excellence in Advanced Materials and Green Technologies (CoE-AMGT), Amrita School of Engineering, Amrita Vishwa Vidyapeetham, Coimbatore 641112, India

P. K. Akhilesh · A. Vlad

Institute of Condensed Matter and Nanosciences, Universitécatholique de Louvain, 1348 Ottignies-Louvain-La-Neuve, Belgium

P. Raghavan

Materials Science and NanoEngineering Lab (MSNE-Lab), Department of Polymer Science and Rubber Technology, Cochin University of Science and Technology (CUSAT), Cochin 682022, India

Department of Materials Engineering and Convergence Technology, Gyeongsang National University, 501 Jinju-Daero, Jinju 52828, Republic of Korea

Keywords Polymer nanodielectrics · Dielectric properties · Ceramic nanoparticles · Conducting nanoparticles · Applications

5.1 Polymer Nanodielectrics: An Introduction

Polymer nanodielectric composites comprise a polymer matrix and a nanodimensional filler that has at least one dimension in the range of less than 100 nm. Polymer nanodielectrics combine the high breakdown strength and low loss of the polymer matrix with favourable dielectric properties like high dielectric constant of the nanofillers [1]. Due to their nanometric size and high specific surface area of nanoparticles that create large interfacial interactions, they exhibit exceptional properties compared to bulk materials [2]. A schematic representation of the polymer nanodielectric composite and microstructural appearance—correlation between a number of particles and size of particles and the nanoparticle–polymer interface is provided in Fig. 5.1. There are opportunities to tailor nanodielectrics to have a unique combination of properties by careful selection of materials along with engineering the dispersion and interface between the constituent materials. The interfacial region becomes significant as particle size reduces and constitutes a considerable fraction of the polymer dielectric, even at low concentration of the nanoparticle. Hence, it is important to design and optimise the dispersion of nanoparticle in the polymer matrix and the interfacial region to achieve desirable properties. There are various methods reported to prepare nanodielectrics. The popular preparation methods of nanodielectrics composites are depicted below in Fig. 5.2a.

The intrinsic interfacial region can be engineered by changes in matrix structure, mobility, and crosslinking of polymer chains while the extrinsic interfacial regions can be modified by ligands on nanoparticle surfaces resulting from functionalization [3]. Due to these features, nanodielectrics have immense potential in various fields ranging from high-voltage insulation to energy storage devices and sensors.

There are several properties of interest for polymer dielectrics viz. dielectric permittivity, dielectric breakdown strength, dielectric constant, energy density, partial discharge resistance, treeing lifetime, space charge density, tracking resistance, and conductivity [4, 5]. The major factors affecting the performance of nanodielectrics are presented in Fig. 5.2b. Over the past three decades, studies have been conducted on nanodielectrics with different polymers as matrices. They include epoxy resins, polyolefins, polyesters, polyimides, polyimide-amides, polyesterimide, and elastomers. Several nanoparticles are used in polymer nanodielectrics like layered silicates, silicon dioxide, titanium dioxide, aluminium oxide, silicon carbide, barium titanate, magnesium dioxide, zinc oxide, zirconium dioxide, manganese sulphoselenide, etc. [4–10]. The changes in the properties of nanodielectrics upon incorporation of nanofillers vary depending on the nanofiller properties, dispersion, and polymer–filler interaction. In general, it has been observed that the breakdown strength, tracking resistance, partial discharge resistance, tree inception, and growth time are enhanced while space charge accumulation is decreased. However, the effect

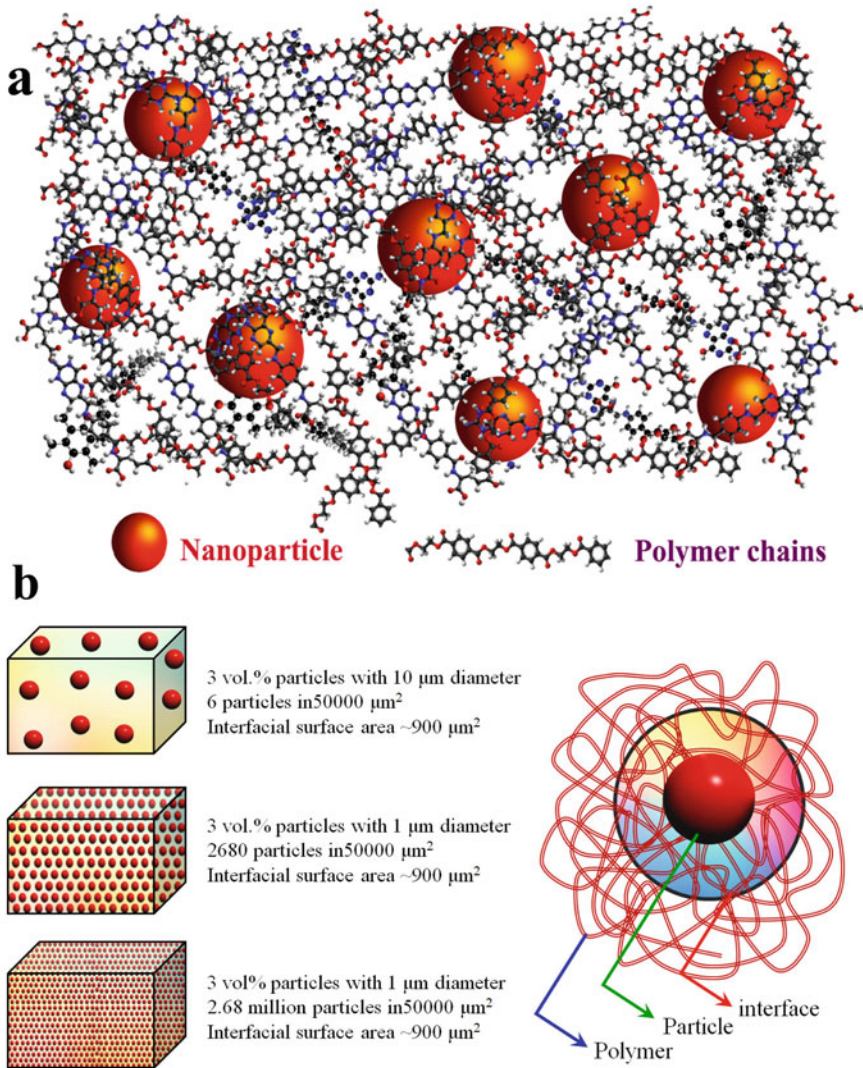


Fig. 5.1 **a** Schematic representation of polymer nanodielectric composite, **b** microstructural appearance—correlation between number of particles and size of particles and the nanoparticle—polymer interface

on properties like permittivity, dielectric loss, and DC conductivity are complicated and may increase or decrease depending on several factors [5]. This chapter examines the current developments in nanodielectric composites for energy storage applications with an emphasis on fundamental material concerns for two different types of polymer nanodielectrics: composites of polymer and ceramic and conductive

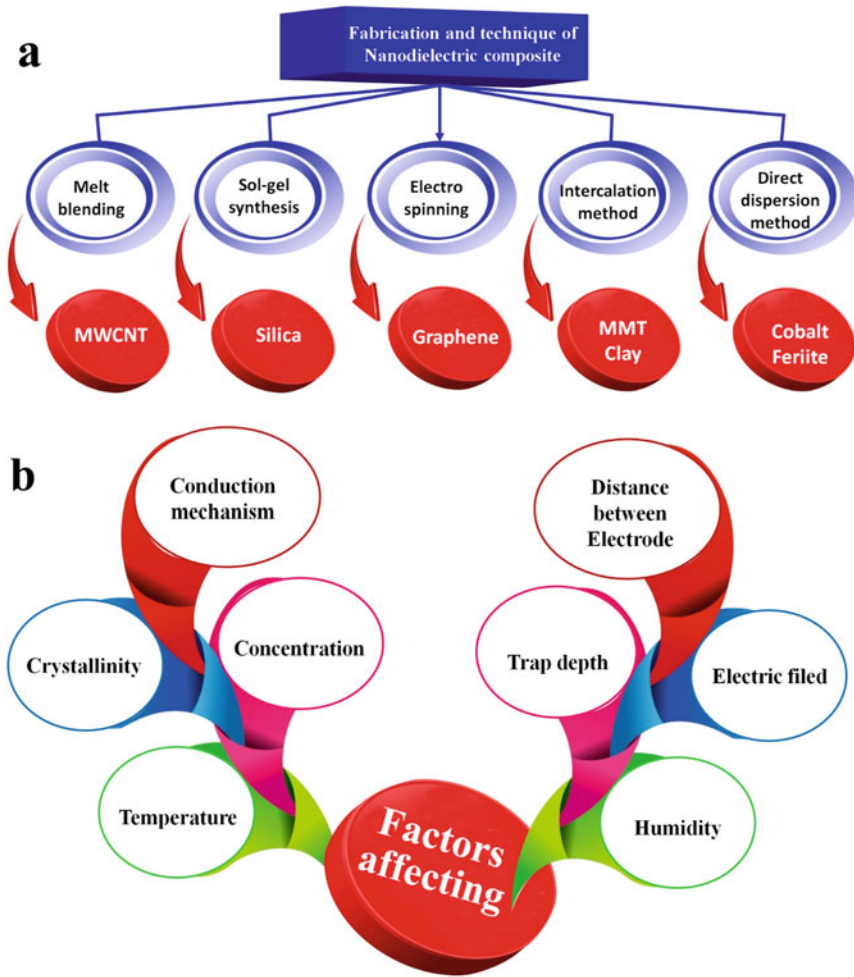


Fig. 5.2 **a** Various fabrication methods for synthesising nanodielectrics and **b** the major factors affecting the performance of nanodielectrics

nanoparticles. The applications, opportunities, and challenges associated with the future developments in nanodielectrics are also discussed.

5.2 Polymer Nanodielectrics Based on Ceramic Nanoparticles

A synergy between high breakdown strength of polymers and high permittivity of ceramic materials can be achieved by choosing specific ceramic materials having architecture surface morphology and particle size to be incorporated into the polymer matrix. Sintered bulk ceramics like ferroelectric BaTiO₃ possess relative permittivity (ϵ_r) higher than 1000 in value. By reducing the internal strain energy and electrostatic energy of jammed crystalline grains, bulk BaTiO₃ with polygrain has been shown to have ferroelectric domains of 180° orientation and domains of 90° for tetragonal phase [11].

In a study by Paniagua et al., phosphonic acid was adopted as a surface initiator for the formation of polystyrene and polymethylmethacrylate (PMMA) over the barium titanate (BTO) nanoparticles via atom transfer radical polymerization. This method of preparation resulted in BaTiO₃ as a core embedded in the grafted polymer as shown in Fig. 5.3a. The surface morphology of the resulting polymer nanodielectric composites is displayed in Fig. 5.3b–e. The performance evaluation at a field strength of ~ 220 V/ μm showed that the one-component system, (PMMA-grafted-BTO) exhibited a maximum extractable energy density (2 J/cm³), which was two times higher than that of the composite without covalent attachment or the pristine polymer. Due to the high permittivity, high breakdown strength, mechanical flexibility of the nanoparticles, and ease of processability due to the organic polymer, such materials have potential applications in hybrid capacitors [12].

The ability of a substance to store electrical energy in an electrical field is measured by a number called the dielectric constant, which is the relative permittivity of a dielectric material. Due to the absence of grain boundaries in ceramics, it is possible to enhance the dielectric characteristics of polymers by using carefully chosen nanoceramic fillers. The relationship between breakdown strength and dielectric permittivity of various dielectric materials is displayed in Fig. 5.4.

Higher ϵ_r values are caused by ionic polarisation between ferroelectric domains and movable domain walls in ferroelectric ceramics². Because of the large domains, which lessen the number of domain walls, ϵ_r is not particularly high for bulk BaTiO₃ when grain size is above 1 μm . The greatest value of ϵ_r was reported to be ~ 5000 with a large number of relatively tiny domains, and when ϵ_r value continued to decrease, such as by 30 nm, it was reported to be ~ 1000 [11, 13, 14].

For BaTiO₃ particles that are nanosized, the ϵ_r value depends on both the synthesis methods used to create the nano-BaTiO₃ particles as well as the ferroelectric and paraelectric phases. Nanoparticles typically do not undergo the effects of sintering at high temperature, but they do exhibit a variety of crystallographic flaws, e.g. BaTiO₃ nanoparticles in the ferroelectric-tetragonal phase have a greater ϵ_r value compared to those in the paraelectric-cubic phase. Paraelectric BaTiO₃ nanoparticles with a size of less than 200 nm are typically produced using low temperature hydrothermal and sol–gel methods, whereas ferroelectric BaTiO₃ nanoparticles larger than 200 nm are typically produced using high-temperature pyrolysis and combustion methods. Since

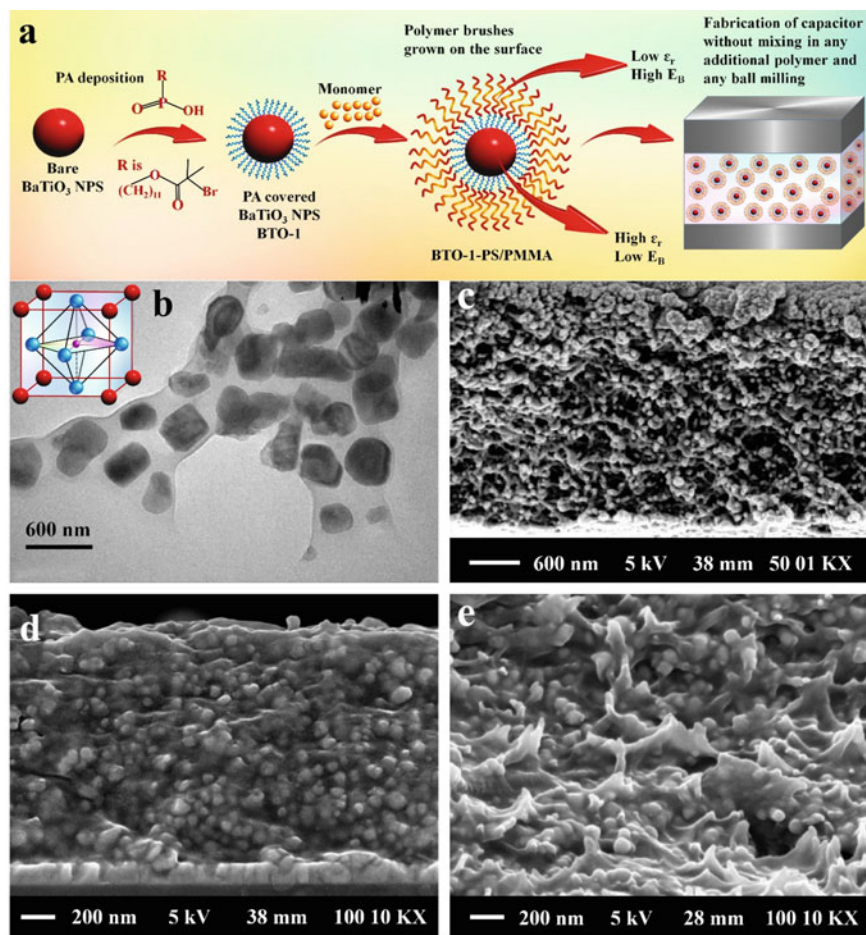


Fig. 5.3 a Scheme for the creation of a one-component, three-constituent hybrid dielectric that can be used to build capacitors. b TEM micrograph of BTO-1-PS composite [29% (v/v) BTO] (inset: crystal structure of BaTiO₃) and c cross section SEM image for composite 5 [19% (v/v) BTO], d cross-sectional SEM for composites BTO-1-PMMA and e BTO-1/cPMMA22 (both 22% (v/v) in BTO) [12]. Adapted with permission from ref. [12] Copyright (2014) (American Chemical Society)

it is practically impossible to quantify the ϵ_r value for such tiny particles directly, various mixing procedures have been used to separate nanoparticles from polymer composites. It is usually claimed that the Bruggeman mixing model, which takes into consideration particle–particle dipole interactions, provides a more accurate estimation of ϵ_r for BaTiO₃ nanoparticles than any other model [15]. The ϵ_r value was discovered to drop from 800 to 200 for particle sizes greater than 10 μm , and on further reduction in size, the ϵ_r value was reported to be ~ 50 for 5–20 nm BaTiO₃ nanoparticles [16–18].

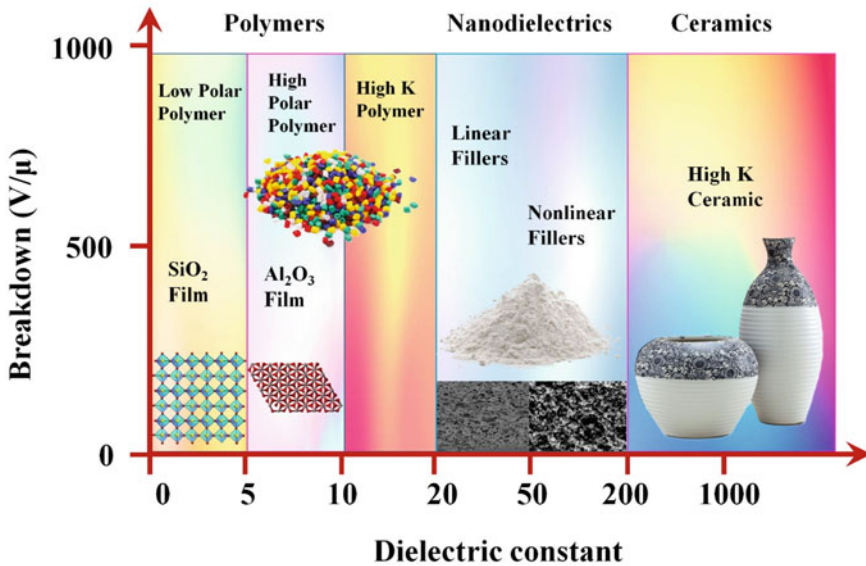


Fig. 5.4 Relationship between breakdown strength and dielectric permittivity (dielectric constant) of various dielectric materials

The crystalline grain and domain structure has a significant impact on the ϵ_r of perovskite nanoparticles. Multiple crystal grains are typically found in one phase of BaTiO₃ nanoparticles larger than 1–10 μm in size, and they typically exhibit the ferroelectric/tetragonal phase, which has 180° and 90° domains at room temperature. They have an extremely high ϵ_r value because 90° domain walls are present. Only single crystal grains were seen as particle size decreased from 0.2 to 1 μm because there was no particle jamming, and therefore, no need for them to minimise internal strain energy. The only 180° domain walls that were present in this kind of single crystal grain structure nullify the impact of the dipoles and cause the ϵ_r to decrease further [19–21].

To achieve uniform dispersion of nanoparticles without blending any homopolymers, polymethyl methacrylate (PMMA) was grafted with 70 nm BaTiO₃ nanoparticles in one experiment. In this experiment, it was found that ϵ_r increased with the BaTiO₃ volume fraction [22]. The maximal ϵ_r in the PVDF/BTO nanocomposite was discovered to be up to 60 vol%, which is three times greater than PVDF in value. ϵ_r began to decline above 60 vol% because of the spin-coated composite film's porosity. The results of the research conclude that compared to polymer matrices, addition of ceramic nanofillers into it enhances the ϵ_r by 3–5 times before percolation threshold is reached [23].

The 1D nanofillers, like nanowires, nanofibers, and nanotubes with higher aspect ratio (AR) were also tested for their effects when added to spherical ceramic nanofillers. It was found that these fillers boost at lower filler contents inside the

ceramic nanofillers [24, 25]. It was discovered that filling the BaTiO₃ with larger aspect ratio nanowires increased the ϵ_r for PVDF at higher filler loadings [26].

The polar coupling contact is stronger in the longitudinal direction compared to the transverse direction (i.e., along the diameter) in high aspect ratio (AR) fillers, and as a result, ϵ_r is higher in the longitudinal direction compared to the transverse direction [26]. Because movable domain walls are present in ferroelectric/tetragonal BaTiO₃ nanotubes and nanowires, it has been found that their ϵ_r is higher than those of paraelectric/cubic nanotubes and nanowires. This suggests that the crystalline phase also affects the ϵ_r s of nanotubes and nanowires [27]. High aspect ratio fillers have a substantially lower percolation threshold than spherical nanoparticles [28]. A parallel capacitor circuit is used to model the overall capacitance when the high aspect ratio nanofillers are oriented to the electric field parallelly, whereas a series circuit is used to model when the nanofillers are perpendicular to electric field.

$$C = C_f + C_m$$

$$\frac{1}{C} = \frac{1}{C_f} + \frac{1}{C_m}$$

where C_f is capacitance for filler and C_m is capacitance for matrix

The parallel capacitor model gives significantly greater ϵ_r , i.e., when the fillers in the composites are oriented parallelly, it gives a greater ϵ_r compare to fillers oriented perpendicular to the applied electric field [29]. For ceramic filler, the ϵ_r 's value is only slightly higher than base polymer when the percolation threshold value is not yet reached. However, above this percolation threshold value, the polymer/ceramic interface acts as a conductive pathway, significantly reducing E_b and η , making it only fit for low-voltage applications. Additionally, polymer nanocomposite materials with ceramic filler loadings greater than 10 vol% are frequently brittle and susceptible to mechanical failure, making them unsuitable for use in film capacitors.

5.2.1 Dielectric Loss

Low dielectric loss is crucial for any practical thin film capacitor application, and the equivalent series resistance provides the total of these various dielectric losses (ESR). As the ripple grows and the ESR rises, wound capacitors heat up significantly, shortening their lifetime [30]. For the deployment of novel polymer dielectrics for thin-film capacitance applications, a low dielectric loss achievement is more crucial than a high U_e since at higher temperatures ripple current heating is unfavourable.

Dielectric losses in polymer nanodielectrics are not only caused by the polymer matrix and ceramic fillers but also due to their interactions. Sources of dielectric losses depend on several polarisation mechanisms [31], including:

- a. Dielectric loss owing to resonant (due to electronic and atomic polarization) and relaxation (due to orientational polarization);
- b. Space charge conduction (due to ions and electrons);
- c. Extrinsic and intrinsic ferroelectric switching of aligned electric domains, the former caused due to impurity ion losses and thermally activated electrons, the latter being a feature of dielectric itself.

Extrinsic dielectric losses in ceramic fillers are caused by lattice vibration in domains, which also causes ionic polarization, and intrinsic dielectric losses in domain walls caused by dipole vibration. Because of the high dipole mobility in the walls, relaxation loss for perovskite crystals occurs around about 1 GHz [13]. Lattice ionic polarisation occurs in ferroelectric domains at 20 GHz frequency [32] that is higher than the power frequency (1 Hz to 1 MHz). Ceramic fillers, therefore, exhibit relatively low intrinsic loss at the power frequency. When it comes to nanoceramic fillers, the leakage current is not significant until the percolation threshold is reached, but above this value, the significance of the leakage current because of the percolated polymer–ceramic particles interfaces under high electric field is enhanced. On the other hand, in case of bulk ceramics, the leakage current due to conduction of electrons originates from grain boundaries causing an extrinsic dielectric loss. The intrinsic and resonant losses occur in the optical ($>10^{14}$ Hz) and infrared (10^{12} – 10^{14} Hz) ranges, respectively. Since the power frequency range is within 10^2 – 10^6 Hz, little resonant loss is always seen. Since polar polymers inherently have larger relaxation dielectric loss than nonpolar polymers, the relaxation loss is placed right inside the power frequency range. When used for high-field poling, ferroelectric polymers like PVDF and its copolymers cause severe hysteresis or ferroelectric loss, which is why they are never used for electric energy storage [33, 34]. Both ionic and electronic currents are large in polymers above T_g/T_m temperature. The extrinsic dielectric loss due to impurity ion contamination and thermally activated electrons make them unfavourable candidate for applications of high-voltage capacitors. Compared to a liquid amorphous matrix, polymer crystals are better at preventing the conduction of electrons and ions [35]. Polar polymers typically have impurity ion concentration below trace levels but can be still contaminated at higher temperatures [36, 37].

The E_b for polymer/ceramic particle nanodielectrics is greatly reduced because of the strong interaction between high- κ (dielectric constant) ceramic fillers and polymer matrix. At lower frequencies, an impurity ion conduction loss in the polypropylene matrix of the PP/BTO@POSS nanocomposite was detected, which increased with temperature. The polarisation of thermally activated electrons in BTO nanoparticles is responsible for the rather broad and feeble peak at 1 kHz frequency that was seen. Remarkable hysteresis loss was noted for the PP/BTO@POSS at 20% nanocomposites with input electric fields greater than 50 MV/m. At the same electric field, the above-mentioned nanocomposite displays a higher U_e value than the pristine polypropylene, but the η considerably dropped as a result of the widened hysteresis loop. The conductivities and ϵ_r s of the PP matrix and the BTO fillers differ significantly. BTO has a high thermal conductivity because of its comparatively high ϵ_r , which results in an unusually large concentration of thermally activated electrons.

The highly insulating PP matrix blocks these thermally activated electrons when an electric field is applied, creating interfacial polarisation, because of which, the interfacial charges within the BTO nanoparticle may move back and forth resulting in a great loss of conduction. The contact between BTO and PP and bulk BTO are the two potential conduction paths. Out of these two, the primary conduction pathway is the PP/BTO interface [38]. A thin layer of linear ceramic dielectrics is typically employed such as amorphous SiO_2 , Al_2O_3 , and TiO_3 using techniques like layer-by-layer coating of methyl aluminoxane, sol-gel preparation, or even atomic layer deposition to further reduce the interfacial conduction. Although the amorphous oxide surface coating's highly insulating qualities allowed for a reduction in interface conduction, hysteresis loss persisted.

5.2.2 Dielectric Breakdown Strength

One of the major benefits for films of polymer is their higher dielectric breakdown strength (E_b), and BOPP currently has the highest breakdown strength of all commercially available films (E_b at 63.2% failure probability of ~ 730 MV/m for 2cm^2 sample area) [39]. The E_b value results from the following variables:

- a. PP resins that are ultraclean;
- b. minimal leakage current;
- c. consistent film thickness.

When working at ~ 200 MV/m and 85°C , this high E_b guarantees a continuous lifetime of $> 100,000$ h. The energy bandgap (E_g) of the material strongly influences the intrinsic E_b (E_b is proportional to E_g^α) [40, 41] with $\alpha = 3$ for semiconductors and $\alpha = 1$ for insulators. Due to their wide energy band gap and slow carrier movement, polymers have a high E_b value [42, 43]. The highest observed value of E_b for most insulating polymers is only 750 MV/m, which is due to intrinsic/extrinsic flaws and degradation (such as broken bonds) under high-field stresses [44]. Theoretically, the intrinsic E_b value for PP is larger than 2 GV/m.

The four primary processes for breakdown in any polymer thin film are electronic breakdown, thermal breakdown, electromechanical breakdown, and partial discharges [44]. Low temperatures are necessary for electronic breakdown, and a strong electric field is needed to introduce hot metal electrons into the polymer dielectric [31]. Hot electrons that are injected into a polymer will break chemical bonds to produce Auger electrons, which then disrupt neighbouring molecular bonds [45]. Thermal breakdown in polymer dielectrics occurs via joule heating and typically takes place at higher temperatures with a smaller electric field. At the locations of flaws and impurities in polymers, both breakdown mechanisms cause gas-phase production. Precleaning is used in the film capacitor manufacturing process to minimise these flaws. Distribution of electric field in nonuniform way becomes another crucial element in multicomponent systems because of the significant ϵ_r and conductivity of electrons differences between ceramic fillers and polymer as

matrix. Interfacial polarisation was seen in this type of system along the E_o direction at the two poles of a single particle. Because of the compatibility of the POSS ligand and the polypropylene matrix, the high dielectric constant nanoparticles of BTO dispersed well in the polypropylene /BTO@POSS nanocomposite than in the PP/BTO nanocomposites. The Weibull E_b of the PP/BTO@POSS nanocomposites dramatically lowered as compared to the hot-pressed PP, and as a result of the BTO particles clustering, the PP/BTO nanoparticles had an even lower Weibull E_b . According to the results, it is crucial to distribute ceramic nanoparticles evenly throughout the polymer matrix. The affinity of high dielectric constant particles with the polymer as matrix can be improved by functionalising surfaces of nanofillers with tiny molecules like dopamine, organosilane, and organophosphate ligands, or by grafting polymer brushes. Al_2O_3 , Ta_2O_5 , ZrO_3 , and TiO_2 are some examples of ceramic nanoparticles with a moderate ϵ_r that is utilised to prevent the field concentration caused by increased interfacial polarisation near high- κ particles. Where there is insufficient filler to cause percolation, these high- κ ceramic nanofillers will produce low energy density and a low ϵ_r . Creating nanoparticles with a core-shell morphology that have a gradient ϵ_r profile from the polymer matrix to the core and shell of the nanofillers is an alternative strategy [46]. According to a phase-field modelling when the thickness of the shell is roughly equivalent to the diameter of the core, the ideal core-shell structure is produced [47]. In addition, the distinctive 2D nanofillers of plate-like structure offers a stronger capability of blocking charges to impede movement of electrons within the nanocomposite. Low level of filler can minimise filler agglomeration and hence concentration of local fields. When ultrathin boron nitride nanosheets (BNNS) were used as filler in P(VDF-TrFE) in trials, the E_b value was recorded as 610 MV/m, which was a 70% increase over the E_b value of the film with a pristine PVDF-TrFE solution-cast sample (362 MV/m) [48].

Nanoparticles have large surface area, which cause lot of flaws on their surfaces. These flaws also could be caused by foreign atoms on the surface, irregularities in the surface's geometry, or the molecules close to the particle's surface being non-centrosymmetric (coordinative unsaturation) [49]. These flaws lead to the generation of new localised energy levels in a band that would otherwise be forbidden. The created energy levels could be charge traps that are located in the band gap between the valence and conduction bands (localised states in the band gap). They prefer to fill these traps rather than remain in the conduction or valence band when mobile charges, such as electrons or holes, are present [50]. Once it has filled the trap, the electron or hole finds it difficult to return to the conduction or valence band, especially if the trap is deep enough; however, it can migrate to nearby similar traps if they are close enough [97].

As seen in Fig. 5.5a, they may transition from one particle interphase to another. This could worsen the characteristics of electrical insulation and promote charge mobility in nanocomposites. If the traps are deep enough and far from each other, these phenomenon will not take place. In contrast, if the aforementioned defects produce energy states that are deeper in the conduction/valence band, this may enlarge the band gap in the particle interphase region and act as an energy barrier for the passage of charges. These phenomenon is schematically displayed in Fig. 5.5b. This

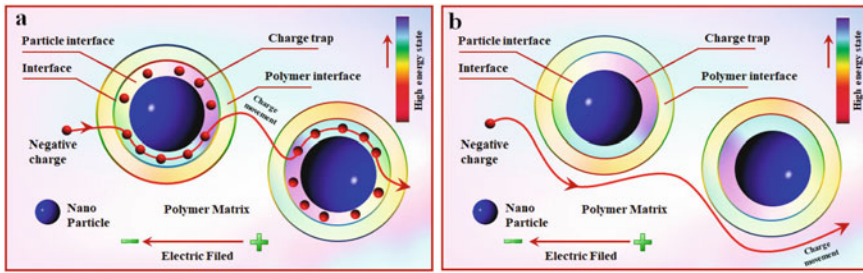


Fig. 5.5 **a** Possible mechanism for charge movement through the charge traps in the particle interphase and **b** the particle interphase represents an energy barrier for charge movement [49]. Adapted with permission from ref. [49] Copyright (2018) (Elsevier)

may indicate a potential mechanism that enhances the nanocomposites' dielectric characteristics.

A novel method of stacked nanodielectrics has been developed by researchers to enhance both E_b and ϵ_r of nanocomposites [51]. The fundamental idea behind this technique is to produce a dielectric “hard” layer with a high E_b and a dielectric “soft” layer with a high ϵ_r in a rationally constructed film architecture. A small percentage of insulating nanofillers are present in the high E_b layer, whereas the high- κ layer contains a substantial number of high- κ fillers. To maximise the U_e and enhance the synergy between E_b and ϵ_r , tuning is required for the stacked nanodielectrics' architecture, volume percentage, and number of layers.

5.2.3 Discharged (U_e)

In general, raising either ϵ_r or electric field or both can result in a high U_e . Since the power frequency has no resonance losses region, improving electric and atomic polarisation is the best way to boost ϵ_r [42]. When E_g is above 4 eV for insulating polymers, the deformation $\epsilon_{r,s}$ of the polymer cannot exceed 5. This is because of the molecular bonding of localised electrons and atoms. In order to increase the ϵ_r for polymers, orientational and interfacial polarizations are applied; however, they result in dielectric losses in the power frequency. It is not possible to simultaneously increase ϵ_r/U_r and E_b for this reason. Therefore, we are limited to finding an ϵ_r/U_e and E_b compromise. Therefore, for polymer nanodielectrics, getting high U_e should not be as important as obtaining low loss and high E_b . Low dielectric loss is ensured, and U_e should be evaluated at appropriate temperatures and electric fields to actual application. A trilayer BNNS-BT-BNNS structure and stacked c-BCB nanodielectric demonstrated a U_e of 1.1 J/cm³ at a η of 93% at 150 °C and 200 MV/m, which was around 2.8 times that of BOPP seen at 70 °C [52].

Dielectric properties estimation of nanodielectric interphase by numerical modelling and dielectric spectroscopy is studied by Andrei et al. [53]. In their

studies, to calculate the frequency-dependent dielectric properties of the polymer-nanoparticle interphase, an electro-quasistatic numerical model of a PP-SiO₂ nanodielectric is suggested. It is based on a combination of dielectric spectroscopic results and semi-analytical formulations. The nanodielectric model is made up of spherical SiO₂ nanoparticles with a diameter of 15 nm that are evenly dispersed across a PP matrix. Each nanoparticle is encircled by an interphase that is 10 nm thick.

5.3 Polymer Nanodielectrics Based on Conductive Nanoparticles

Metallic and conductive nanoparticles [54] and carbonaceous nanoparticles (such as carbon black (CB) [55], carbon nanotubes (CNTs) [56], and graphene nanoplates (GNPs) [57]) are utilised as fillers in polymer nanodielectrics. When a polymer serves as the matrix, the conductive particles become polarised when an electric field is applied, and this causes the internal electric field to be zero.

When linear dielectric regime as determined by broadband dielectric spectroscopy (BDS), the great dielectric constant has been reported for some of these nanodielectrics in recent years, e.g. adding Ag nanoparticles as filler to epoxy could result in a relative dielectric constant (ϵ_r) of more than 300 [54].

Conductive particles in thin polymers function as nanoscale electrodes, and nanocapacitors are created at the interface between the polymer and the nanoparticles. The percolation barrier is nearly reached when the filler material, the connection between nanocapacitors to one another as well as to metal electrodes [57]. A high $\epsilon_{r,\text{app}}$ (colossal apparent) occurs when the thickness or interparticle distance of the boundary layer becomes very tiny. Since there is no conduction or tunnelling of electrons at low fields (<1 MV/m), the $\tan \delta$ value for these nanodielectrics likewise stays low.

Large ceramic granules that are semiconductive and thin insulating grains borders form the grain boundary barrier layer (GBBL) in ceramic capacitors, and their polarisation results in a colossal apparent ($\epsilon_{r,\text{app}}$) resistance of up to 10⁵ [58] which is given by,

$$\epsilon_{r,\text{app}} = \frac{\epsilon_{gb}d_g}{t}$$

where ϵ_{gb} is dielectric constant of insulating grain boundary layer, d_g is average grain size of dielectric material, and t is thickness of insulating grain boundary layer.

Local electron tunnelling is provided at the grain boundaries via a Schottky barrier. In order to prevent charges from being injected via the conductive medium, from metal electrodes to bulk composite channel, it is crucial to ensure that there will be no direct contact between the metallic electrodes and semiconducting granules [59]. Researchers used nanosized (18 and 100 nm) surface functionalised aluminium nanoparticles using polymer brushes and a matrix made of isotactic polypropylene

(iPP) to study the improvement of dielectric constant by incorporating nanosized conductive particles into polymer/conductive particle nanodielectrics. The ϵ_r of PP/nAl nanodielectrics was investigated using BDS at various nAl concentrations under an applied electric field of 1MV/m. It was found that the $\epsilon_{r,app}$ was only 5.7 at 25 vol% of 100 nm nAl, which was 2.5% less than iPP [60].

Conductive electrons may tunnel into the polypropylene matrix in the presence of strong electric fields, causing dielectric loss. Due to conduction loss, these injected electrons also significantly reduce the E_b (breakdown strength) of polymer/conductive particle nanodielectrics. This was seen in an experiment where E_b was reduced from 620 MV/m for iPP on 5 vol% nAl to 300 MV/m on 25 vol% loading. When metallic nanoparticles are polarised, the charges in the interfacial region cause a strong change in the polymer matrix's local electric field in the direction of the electric field. These close-by areas cause dielectric breakdown and electron tunnelling in the iPP matrix, making them hot spots.

Therefore, under an elevated local field, the metallic particles transform into providing free electrons to the PP matrix by electron sources via electron tunnelling, making nanocomposite conductive above a particular threshold, ultimately resulting in catastrophic dielectric breakdown. The increase of $\epsilon_{r,s}$ in polymer nanodielectrics is facilitated by these kinds of electrons conducting under a strong electric field. Because the internal electric field for metallic particles in conductive nanoparticle nanodielectrics is laterally zero, they are unable to store any electric energy. As a result, the augmented ϵ_r and U_r can only be achieved by raising the polymer matrix's local electric field [45].

The metallic particle size must be lower than 2–3 nm at normal temperature to display an efficient Coulomb blockade effect [61], yet it is challenging to disperse these tiny metallic nanoparticles uniformly in the polymer matrix. As a result, high-voltage capacitor applications cannot use composites of polymer and metallic nanoparticles.

Due to their high aspect ratio, CNTs and GNPs can easily aggregate or percolate when used as fillers, which increases the conductivity of polymer/CNT and polymer/GNP nanocomposites. Again, this behaviour led to a situation where conductive pathways transported electrons from the filler to the polymer matrix, increasing the ϵ_{eff} for those nanodielectrics. Regarding a PVDF/GNP nanocomposite made of polyvinylidene fluoride, researchers obtained more than 200 and 2700 $\epsilon_{r,s}$ values at 1000 and 100 Hz, respectively [62]. Additionally, in polymer/carbon nanodielectrics, researchers noticed a nonlinear behaviour in the link between current and voltage [63].

Researchers have suggested a variety of additional methods to increase E_b and decrease conductive filler/polymer nanocomposites' dielectric loss, including a third filler, sandwich/multi-layered buildings, as well as surface coating. One research team created polyurethane (PU) nanocomposites based on CNT fillers with GO capsulation, where the function of the Go was to support the CNT dispersion by π - π interaction and serve as a barrier to prevent direct contact between two CNT particles [64]. As a result, this nanocomposite was found to have a resistivity that was almost four times as high as nanocomposite with CNT-only fillers and to have

no electric percolation. In that experiment, the E_b value was reported at 120 MV/m, substantially doubling its previous value, and it declined as the filler quantity rose. In a further set of experiments, PI-(PI/NH₂-MWCNT)-PI-three-layered films in which the insulating layers block the conductive paths were made resulting in ultralow dielectric loss and high dielectric constant [65]. There were not colossal ϵ_r values reported between 0 and 20 wt% filler content; however, this three-layer film reduced E_b values 300 to 75 MV/m at a 20 weight percent loading, which was better than a single-layer composite of PI and CNT.

5.4 Applications of Nanodielectrics

The advantages of nanodielectrics are excellent mechanical properties, high dielectric breakdown strength, low dielectric loss, high power and energy density, and good processibility. Multiscale models and design methodologies are needed to be compliant for nanodielectrics to be applicable in the industry. Not only to control the dispersion of nanodielectrics, understand the interface contributions, and measuring ageing, there should have necessary tools that will enable customization of the constituent properties to meet the needs of the bulk material for a particular application [4]. These properties of nanodielectrics have been successfully used in many areas such as space charge suppression, high energy density storage in capacitors, generators and motors, wire enamels, and in high thermal conductivity. The selected applications of nanodielectrics are shown in Fig. 5.6.

5.4.1 Space Charge Suppression

The superior characteristics of nanodielectrics reduce the internal electric field in them. The breakdown properties and the anti-ageing capabilities of nanodielectrics can be enhanced, especially in direct current (HDVC) cable operating voltage level and high voltage [66]. Improvement of breakdown strength originates from the interfacial zones formed around the nanoparticles and these zones can modify the trap properties, carrier mobility and charge injection in polymer matrices by changing the chain conformation, aggregation structure, or morphology. These modifications can cause the suppression of space charge accumulation as well as improvement of electrical breakdown strength. By the addition of nanoparticles in the polymer matrix, some nanodielectrics exhibit smaller space charge accumulation. The injected charge is captured by the traps which are formed as the result of the introduction of nanoparticles. This is effective only at lower concentration, and higher charge injection causes the degradation of polymer chains. It has been showed by the various research that the addition of inorganic particles into the polymer matrix can prevent the injection and space charge suppression [67]. Zhang et al. addressed the issue by attaching matrix-compatible polymer brushes to spherical colloidal SiO₂ NPs (10–15 nm diameter) to

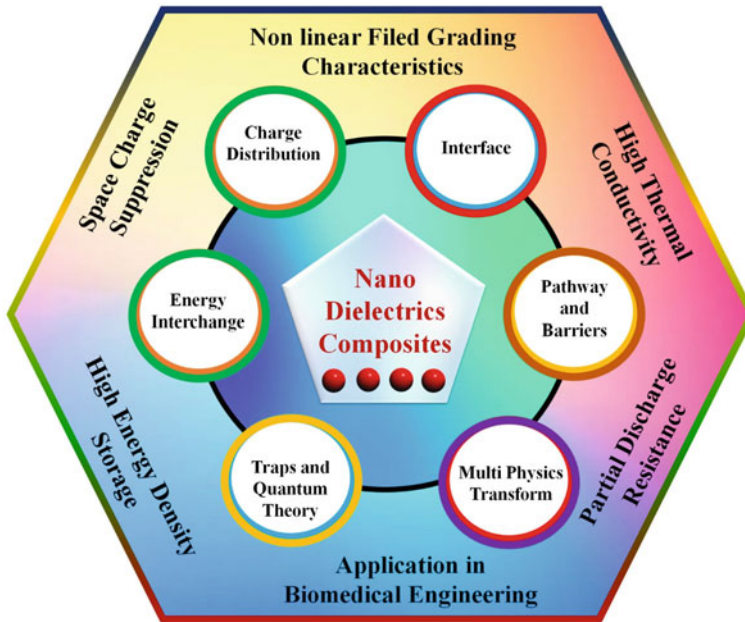


Fig. 5.6 Selected applications of nanodielectrics in various fields

create a uniform NP dispersion in cross-linked polyethylene and were able to achieve improved space charge suppression, improved DC breakdown strength, and limited internal field distortion (10.6%) over a broad range of external DC fields from 30 to 100 kV/mm at room temperature [68]. Zhang et al. in their study showed that the introduction of MgO nanoparticles in low-density polyethylene (LDPE) improved the average trap depth in MgO/low-density polyethylene (LDPE) nanodielectrics. As a result, there was a significant build-up of space charge close to the electrodes. This was measured by using improved pulsed electro-acoustic (PEA) system [69]. Wang et al. evaluated the impact of vinyl silane coupling agent on the electrical characteristics of Al_2O_3 /LDPE nanodielectrics and came to the conclusion that the modified Al_2O_3 nanoparticles have a greater space charge suppressing effect than the unmodified ones [70]. In addition to that, Zhou et al. studied the morphology, dielectric properties, DC volume resistivity, and space charge behaviour of surface modified MgO, TiO_2 , ZnO, and Al_2O_3 blended with polypropylene (PP). The results show that the space charge suppression and breakdown strength first increase with the increase in nanoparticle content and then decreases [71].

5.4.2 High-Density Energy Storage

Polymer-based nanocomposites with high permittivity, high breakdown strength, flexibility, and lower cost are required for deployment in distributed power production systems and high compact electronic circuits [66]. Development of nanodielectric materials is closely related to the advancement of capacitor technology, and it is shown in Fig. 5.7. Polymers serving as the matrix and the fillers are used to increase the effective dielectric constant. Capacitors that can store a higher amount of energy and capable of instantly releasing it are becoming more and more necessary. These capacitors are used in a variety of military and commercial applications. For such applications, a base polymer with a high permittivity, such as poly(vinylidene fluoride) (PVDF), is a good choice to start. In theory, the fillers aid to increase the effective dielectric constant of the system while maintaining the polymer's built in resistance to disintegration. Many studies are reported on the breakdown strength and composite dielectric permittivity of polymer nanocomposites. Most of the research concentrate on improving the dielectric permittivity by using ferro-metal oxides such as $\text{Pb}(\text{Zr}, \text{Ti})\text{O}_3$ (PZT), $\text{Pb}(\text{Mg}_{0.33}\text{Nb}_{0.77})\text{O}_3$ - PbTiO_3 (PMNT), and BaTiO_3 (BT). Studies show that the dielectric permittivity of ceramics can be extended from tens (TiO_2 , Al_2O_3) to thousands (BaTiO_3), and can even can extend to over 10,000 for $\text{CaCu}_3\text{Ti}_4\text{O}_{12}$ [72]. In conductive polymer nanocomposites for high energy density applications, several studies on percolation phenomenon that occurs when the volume percent of fillers exceeds the percolation threshold have been reported [73]. Metal particles, carbon nanotubes, and graphene sheets are used as the conductive fillers. Their polymer-based nanocomposites indicate an exponential increase in permittivity around the percolation threshold. Additionally, a hierarchical structure for nanocomposites has been devised to concurrently increase the breakdown strength and permittivity [74]. Flexible nanocomposites containing polymer and high dielectric ceramic nanoparticles have gained greater importance for dielectric and energy storage application. A core-shell $\text{Ag@polydopamine@BaTiO}_3$ nanocomposites with strawberry-like properties was created by Yang et al. The strawberry-like BT-PDA-Ag show greater enhanced energy density and can be used for energy storage [75]. Wang et al. created a dielectric composite material with extremely high discharge energy density by changing the interface between nanoparticles and poly(vinylidene fluoride-co-hexafluoropropylene) (PVDF-HFP). After coating SiO_2 outside, barium titanate dielectric concentration and current density inside BT particles decrease. This coating with PDA increases the interface interactions with the nanoparticles, and as a result, ultra-high discharge energy has been achieved. With varied BaTiO_3 compositions steadily increasing layer by layer in the nanocomposites, Wang et al. created a new sandwich-like three-layer structure for them [76]. Luo et al. created a 3-D BaTiO_3 network in polymer composite with increased permittivity and energy storage density [77].

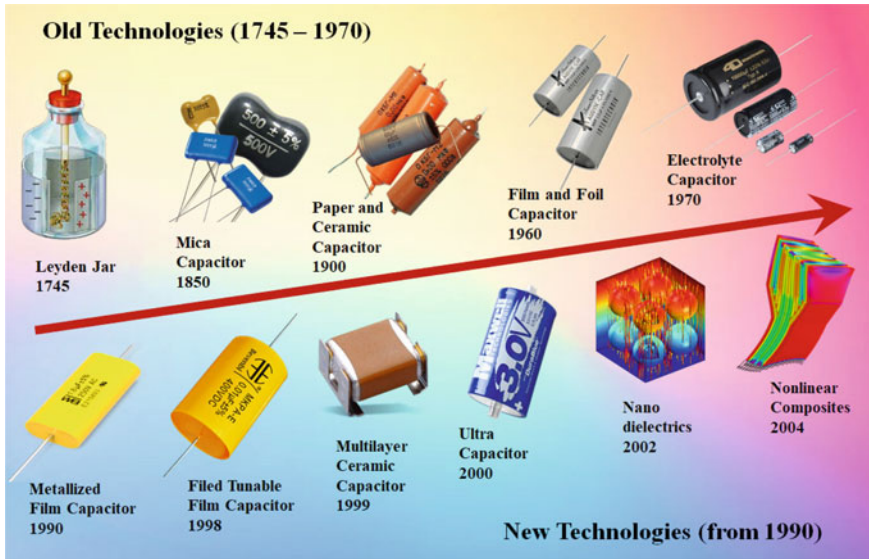


Fig55..7 Development of materials is closely related to the advancement of capacitor technology

5.4.3 Generators and Motors

In rotating machines, it is desirable to have higher capability of withstanding electrical and thermal stress along with improved thermal conductivity [78]. The main advantages of generators are good mechanical strength and environmentally friendly [79]. This was one of the first application of nanodielectric and driving force for improvements in motor systems. Research has been carried out with materials like mica, epoxy resin, and fibre glass. Mica can split in way to form a thin, flat laminate [80], with excellent dielectric qualities, low dielectric losses, heat resistance, and high dielectric strength. High-voltage rotating machines experience the combined effect of thermal, electrical, and mechanical loads. The improvement of voltage endurance is arguably one of the biggest advantages of nanodielectrics [4]. The observed improvement in the short-term AC breakdown strength of roughly 30% opens the door to the possibility of raising working electric stress and/or decreasing ground wall dimensions [81]. The ground wall insulation of large form-wound generators and motors, for which voltage endurance is essential and standards are available, is thus obviously a top target application [82]. Generator design and development is undergoing radical change, not only in the hardware that is being designed but in the way in which they are designed. To meet current and future market demands, improved generator design solutions are required due to the highly flexible peak load regime and the decreasing energy price at the liberalised market. The use of nanoparticles can improve the properties of the dielectrics. A study done on using SiO_2 nanoparticles in epoxy mica has led to a more efficient stator winding insulation system that is

customised to the needs of the new, highly flexible grid without sacrificing longevity on the one hand and the specific power output on the other. In the near future, it might be applied to both new-generation designs and the renovation and upgrading of already installed generators [83].

5.4.4 Application in Wire Enamels

Wire enamels also benefit from nanodielectrics' ability to withstand electrical stress for an extended period. This suggests a way to prepare insulating materials that are resistant to coronas, along with the regularly reported improvement in erosion-resistant under stress [4]. A common low-voltage generator was constructed using stator coils with many turns, ranging from one to sixteen turns per coil which can be random wound or form wound. Random-wound coil generators can be made at low cost, and through the application of vacuum-pressure impregnation, their ability to survive harsh weather conditions can be increased. The low-voltage motors coated with polymer nanocomposites have many applications. When the low-voltage motors are random wound with round wire and coated with polyamide-imide, it offers the necessary abrasion resistance for winding at high working temperatures. The middle layers contain different nanosized oxide fillers, including tin oxide, which was thought to be the most prevalent filler, for increased resistance to partial discharge. Normally, production with greater filler loading reduced wire flexibility, which caused enamel cracks, whereas resistance to partial discharge rose with filler loading. The resistance to partial discharges was considerably enhanced at modest filler loading. Strands of magnet wire with a rectangular cross-section coiled around it puncture the coils for medium- to high-voltage motors. Depending on the magnetic wire's application and type, it goes through the coating a number of times. Here, the construction is layer-by-layer coating which results in multiple polymers to polymer interface. These wound coil wire enamels are applicable in transformers, motors, coils, low-current cables, and telephone installations. Random-wound conductors, which use enamelled magnet wire, are particularly common in the design of tiny motors (and other devices like solenoids) [78].

5.4.5 Nanodielectrics with High Thermal Conductivity

The dissipation from the leakage current grows in the high-voltage field as the level of conducting voltage rises. As electronic components are arranged in integrated circuits with ever-increasing compactness, there is a corresponding increase in heat generation per unit volume. The electrical power system and electronic system needs high thermal conductivity and excellent electrical insulation [66]. There are different types of fillers that can increase the thermal conductivity of nanocomposites [84]. These fillers can be metals, inorganic particles, and carbon materials. Wu et al.

studied the improvement of dielectric properties, high dielectric constant, and low dielectric loss and thermal conductivity nanocomposites utilised in film capacitors for energy storage [85]. Seyhan et al. showed that the thermal conductivity of polymer nanocomposites with boron nitride nanosheets (BNNSs) can be improved while maintaining the characteristics of electrical insulation [86]. Zhang et al. created a nanocomposite of uniformly dispersed strongly orientated graphite in a polymer matrix [87]. Sun et al. added a small amount of silver nanoparticles in order to reduce the interfacial thermal resistance between adjacent BNNSs [88]. Hong et al. created a method to construct 3D hexagonal boron nitride network in a polymer composite which is verified with high thermally conductive and mechanically stretchable [89].

5.5 Future Prospects

5.5.1 *Self-Healing Dielectrics*

It is desirable to have electrical insulation that has self-healing capacity, and it is especially attractive if healing is not dependent on an external source. One such approach is to incorporate encapsulated fluids that are discharged owing to damage and locally cross-link to perform mechanical repair [90]. One illustration of this is the well-known clearing phenomenon built into the metallised film capacitors.

Partial discharges, such those that take place in voids, are cause of majority of localised damage in high-voltage insulation. These discharges also involve the release of photon energy at a precise site where healing is required and can serve as the foundation for a focused self-healing approach. A means of introducing active substances at the interior of the polymer matrix is provided by the insertion of nanoparticles. When these active agents are photosensitive, the energy formed by the light-emitting process can be utilised. Despite being an active field, high-voltage dielectric structures hardly ever use it [4]. However, in recent times, efforts are being made to apply the chemistry and theories of self-healing phenomenon to electrically insulating materials, including methods that use plasma energy.

5.5.2 *Increased Stress Applications*

Any practice use of solid dielectrics is to prevent electrical trembling that results from such as in. In cast spacers for gas-insulated equipment, moulded bushings, and cast transformers, one of the problems limiting their durability is electrical treeing caused due to electrical stresses. Electrical treeing is caused due to electrical stresses developed in the material that arises from defects arising in moulding processes like in extrusions, moulding, or casting. Hence, the average stress inside the material is to be kept at low level. Nanomaterials dispersed in polymer dielectric act as barrier

that slow the formation of trees and enhances the resistance of materials to electrical treeing in a wide variety of materials [8, 10, 91]. The dielectric strength of HVDC cables is significantly influenced by charge injection, trapping, and space charge accumulation [92]. In XLPE-nanoclay composites, the stress concentration was found to be maximum at the interface of nanoclay and XLPE, while stress concentration inside the nanoclay platelet was lower. The tortuous path created by dispersed nanoclay in XLPE prevented the propagation of both electrical treeing and water tree [10]. Conducting nanosized fillers improve electrical conductivity, which lowers the tendency of materials to accumulate charge [93].

5.5.3 *Biomedical Applications*

When activated by an outside electric field, flexible materials known as electroactive polymers (EAP) show a change in size or shape. Dielectric elastomers (DEs), a type of EAP, are representative of potential applications ranging from artificial muscle to robotics interaction due to their satisfied mechanical and dielectric properties, such as lightness, softness, flexibility, high deformability, quick response, and low cost [94]. Wang et al. investigated dielectric elastomer nanocomposites with multi-walled CNT and concluded that the electric fields inside the material are concurrently decreased and the deforming performance is improved [95]. A fascinating experiment by Kwak et al. used artificial muscle based on DE to simulate human facial expressions on a robot [96]. In addition to their employment in artificial muscles, these soft dielectric materials' electromechanical capabilities are frequently employed as functional sensors to pick up on environmental changes or human motion. Chhetry et al. stated that the strategy of the microstructuring dielectric material is leveraging the sensor's performance by enhancing the effective permittivity and reducing the stiffness [97].

5.6 Challenges and Future Trends

In this chapter, we have discussed about some of the important features of nanodielectrics and the major research related to the applications. Over the past 15 years, researchers in the field of dielectrics have made significant advancements in the manufacturing of nanodielectric films and materials. The knowledge in dielectric polymer and nanodielectric composites have grown as a result of scientific investigation from the atomic scale to the nanometre and micrometre levels and continues to grow in terms of applications. Adopting antiferroelectric fillers and creating atypical composites may result in a high energy density. A potential and workable method for increasing the energy density without reducing the dielectric strength is to keep fillers at a lower loading fraction. It is possible to increase the dielectric strength of dielectric polymers by molecularly altering the chemistry of the polymer; however, this will call for more research and a scale-up procedure. Though film scale-up might be difficult,

the logical design of polymer dielectrics may offer scientific direction for dielectric material synthesis in practice [98]. The most recent advancements in enhancing the dielectric strength of polymer films should be further evaluated on a wide scale and thinner gauges. More research should be done on economical polymers. The current market demands for advanced film capacitors are still uncertain, and the high cost of capacitors makes it difficult to implement new technologies. There should be more research done on polymers with intermediate dielectric constants and polymer composites, like high-temperature polymers that have undergone molecular modification for achieving desired qualities without sacrificing dielectric loss. It is important to continue paying attention to the basic principles of nanodielectrics, polymer chemistry, and computer modelling. In the long run, this will provide superior dielectrics with a high dielectric constant, high dielectric strength, and low dielectric loss [97]. However, overcoming the high cohesive energy of nanoparticles and ensuring homogenous dispersion remains difficult, particularly for production at an industrial scale [66]. The dielectric characteristics of nanoparticles can be effectively improved by surface modification.

References

1. Zhang G, Li Q, Allahyarov E, Li Y, Zhu L (2021) Challenges and opportunities of polymer nanodielectrics for capacitive energy storage. *ACS Appl Mater Interf* 13(32):37939–37960. <https://doi.org/10.1021/acsami.1c04991>
2. Ashok N, Prakash K, Selvakumar D, Balachandran M (2020) Synergistic enhancement of mechanical, viscoelastic, transport, thermal and radiation ageing characteristics through chemically bonded interface in nanosilica reinforced EPDM-CIIR blends. *J Appl Poly Sci* 138(12):50082. <https://doi.org/10.1002/app.20201087>
3. Schadler LS, Nelson JK (2020) Polymer nanodielectrics—short history and future perspective. *J Appl Phys* 128:120902. <https://doi.org/10.1063/5.0019865>
4. Tan DQ (2020) The search for enhanced dielectric strength of polymer-based dielectrics: a focused review on polymer nanocomposites. *J Appl Polym Sci* 137(33):49379. <https://doi.org/10.1002/app.49379>
5. Tanaka T, Imai T (2013) Advances in nanodielectric materials over the past 50 years. *IEEE Elect Insulat Magazine* 29(1):10–23. <https://doi.org/10.1109/MEI.2013.6410535>
6. Yasoda KY, Baji DS, Kumar MS, Santhanagopalan D, Batabyal SK (2023) Sustainable development of manganese sulfoselenide nanoparticles anchored graphene oxide nanocomposite for high-performance supercapacitor and lithium-ion battery applications. *J Alloys Compound* 930:Art. no. 167282. <https://doi.org/10.1016/j.jallcom.2022.167282>
7. Murali B, Baiju KG, Prasad RK, Kumaresan D (2023) Fabrication of barium titanate nanowires-GNP composite bilayer photoanodes for the high-performance dye-sensitized solar cells. *Appl Surf Sci* 610:Art. no. 155316. <https://doi.org/10.1016/j.apsusc.2022.155316>
8. Kavitha D, Sindhu TK, Nambiar TNP (2017) Impact of permittivity and concentration of filler nanoparticles on dielectric properties of polymer nanocomposites. *IET Sci, Measurement Tech* 11(2):179–185. <https://doi.org/10.1049/iet-smt.2016.0226>
9. Sreehitha PR, Durga B, Balachandran M (2020) Dielectric properties, thermal characteristics and degradation kinetics of PMMA nanodielectrics. *Mat Today: Proceed* 24(2):772–781, 17
10. Kavitha D, Balachandran M (2019) XLPE—layered silicate nanocomposites for high voltage insulation applications: mechanical and treeing behavior. *IET Sci, Measure Tech* 13(7):1019–1025. <https://doi.org/10.1049/iet-smt.2018.5417>

11. Buscaglia V, Randall CA (2020) Size and scaling effects in barium titanate. an overview. *J Eur Ceram Soc* 40(11):3744–3758. <https://doi.org/10.1016/j.jeurceramsoc.2020.01.021>
12. Paniagua SA, Kim Y, Henry K, Kumar R, Perry JW, Marder SR (2014) Surface-initiated polymerization from barium titanate nanoparticles for hybrid dielectric capacitors. *ACS Appl Mater Interfaces* 6:3477–3482. <https://doi.org/10.1021/am4056276>
13. Teranishi T, Hoshina T, Tsurumi T (2009) Wide range dielectric spectroscopy on perovskite dielectrics. *Mater Sci Eng B* 161(1–3):55–60. <https://doi.org/10.1016/j.mseb.2008.11.039>
14. Arlt G, Hennings D, de With G (1985) Dielectric properties of fine-grained barium titanate ceramics. *J Appl Phys* 58(4):1619–1625. <https://doi.org/10.1063/1.336051>
15. Allahyarov E, Löwen H, Zhu L (2016) Dipole correlation effects on the local field and the effective dielectric constant in composite dielectrics containing high-k inclusions. *Phys Chem Chem Phys* 18(28):19103–19117. <https://doi.org/10.1039/C6CP03149H>
16. Goswami AK (1969) Dielectric properties of unsintered barium titanate. *J Appl Phys* 40(2):619–624. <https://doi.org/10.1063/1.1657443>
17. Hsiang H-I, Yen F-S (1993) Dielectric properties and ferroelectric domain of BaTiO₃ powders. *J Appl Phys* 32(Part 1, No. 11A):5029–5035. <https://doi.org/10.1143/JJAP.32.5029>
18. Guo HZ, Mudryk Y, Ahmad MI, Pang XC, Zhao L, Akinc M, Pecharsky VK, Bowler N, Lin ZQ, Tan X (2012) Structure evolution and dielectric behavior of polystyrene-capped barium titanate nanoparticles. *J Mater Chem*. <https://doi.org/10.1039/c2jm35600g>
19. Li Y, Liao Z, Fang F, Wang X, Li L, Zhu J (2014) Significant increase of curie temperature in nano-scale BaTiO₃. *Appl Phys Lett* 105(18):182901. <https://doi.org/10.1063/1.4901169>
20. Polking MJ, Han M-G, Yourdkhani A, Petkov V, Kisielowski CF, Volkov VV, Zhu Y, Caruntu G, Paul Alivisatos A, Ramesh R (2012) Ferroelectric order in individual nanometre-scale crystals. *Nat Mater* 11(8):700–709. <https://doi.org/10.1038/nmat3371>
21. Polking MJ (2016) Deciphering the physics and chemistry of perovskites with transmission electron microscopy. *Nanoscale* 8(12):6237–6248. <https://doi.org/10.1039/C5NR06186E>
22. Paniagua SA, Kim Y, Henry K, Kumar R, Perry JW, Marder SR (2014) Surface-initiated polymerization from barium titanate nanoparticles for hybrid dielectric capacitors. *ACS Appl Mater Interfaces* 6(5):3477–3482. <https://doi.org/10.1021/am4056276>
23. Kim P, Doss NM, Tillotson JP, Hotchkiss PJ, Pan M-J, Marder SR, Li J, Calame JP, Perry JW (2009) High energy density nanocomposites based on surface-modified BaTiO₃ and a ferroelectric polymer. *ACS Nano* 3(9):2581–2592. <https://doi.org/10.1021/nn9006412>
24. Zhang H, Marwat MA, Xie B, Ashtar M, Liu K, Zhu Y, Zhang L, Fan P, Samart C, Ye Z (2020) Polymer matrix nanocomposites with 1D ceramic nanofillers for energy storage capacitor applications. *ACS Appl Mater Interfaces* 12(1):1–37. <https://doi.org/10.1021/acsami.9b15005>
25. Pan Z, Zhai J, Shen B (2017) Multilayer hierarchical interfaces with high energy density in polymer nanocomposites composed of BaTiO₃@TiO₂@Al₂O₃ nanofibers. *J Mater Chem A* 5(29):15217–15226. <https://doi.org/10.1039/C7TA03846A>
26. Tang H, Zhou Z, Sodano HA (2014) Relationship between BaTiO₃ nanowire aspect ratio and the dielectric permittivity of nanocomposites. *ACS Appl Mater Interfaces* 6(8):5450–5455. <https://doi.org/10.1021/am405038r>
27. Joshi UA, Yoon S, Baik S, Lee JS (2006) Surfactant-free hydrothermal synthesis of highly tetragonal barium titanate nanowires: a structural investigation. *J Phys Chem B* 110(25):12249–12256. <https://doi.org/10.1021/jp0600110>
28. Calame JP (2006) Finite difference simulations of permittivity and electric field statistics in ceramic-polymer composites for capacitor applications. *J Appl Phys* 99(8):084101. <https://doi.org/10.1063/1.2188032>
29. Tang H, Lin Y, Sodano HA (2012) Enhanced energy storage in nanocomposite capacitors through aligned PZT nanowires by uniaxial strain assembly. *Adv Energy Mater* 2(4):469–476. <https://doi.org/10.1002/aenm.201100543>
30. Makdessi M, Sari A, Venet P, Bevilacqua P, Joubert C (2015) Accelerated ageing of metallized film capacitors under high ripple currents combined with a DC voltage. *IEEE Trans Power Electron* 30(5):2435–2444. <https://doi.org/10.1109/TPEL.2014.2351274>
31. Chi KK (2004) Dielectric phenomena in solids. Elsevier

32. Tsurumi T, Li J, Hoshina T, Kakemoto H, Nakada M, Akedo J (2007) Ultrawide range dielectric spectroscopy of BaTiO₃-based perovskite dielectrics. *Appl Phys Lett* 91(18):182905. <https://doi.org/10.1063/1.2804570>
33. Zhu L, Wang Q (2012) Novel ferroelectric polymers for high energy density and low loss dielectrics. *Macromolecules* 45(7):2937–2954. <https://doi.org/10.1021/ma2024057>
34. Soulestin T, Ladmiral V, Santos FDD, Améduri B (2017) Vinylidene fluoride- and trifluoroethylene-containing fluorinated electroactive copolymers. How does chemistry impact properties? *Prog Polym Sci* 72:16–60. <https://doi.org/10.1016/j.progpolymsci.2017.04.004>
35. Li Y, Makita Y, Zhang G, Rui G, Li Z-M, Zhong G-J, Miyoshi T, Huang H-D, Zhu L (2020) Effects of rigid amorphous fraction and lamellar crystal orientation on electrical insulation of poly(ethylene terephthalate) films. *Macromolecules* 53(10):3967–3977. <https://doi.org/10.1021/acs.macromol.0c00646>
36. Chen X, Allahyarov E, Li Q, Langhe D, Ponting M, Schuele DE, Baer E, Zhu L (2020) Reducing dielectric loss by nanoconfined impurity ion transport in multilayer films under low electric fields. *Compos Part B Eng* 190:107908. <https://doi.org/10.1016/j.compositesb.2020.107908>
37. Chen X, Allahyarov E, Langhe D, Ponting M, Li R, Fukuto M, Schuele DE, Baer E, Zhu L (2020) Reducing dielectric loss and enhancing electrical insulation for multilayer polymer films by nanoconfined ion transport under high poling electric fields. *J Mater Chem C* 8(18):6102–6117. <https://doi.org/10.1039/D0TC00522C>
38. Zhang G, Brannum D, Dong D, Tang L, Allahyarov E, Tang S, Kodweis K, Lee J-K, Zhu L (2016) Interfacial polarization-induced loss mechanisms in polypropylene/BaTiO₃ nanocomposite dielectrics. *Chem Mater* 28(13):4646–4660. <https://doi.org/10.1021/acs.chemmater.6b01383>
39. Ho J, Ramprasad R, Boggs S (2007) Effect of alteration of antioxidant by UV treatment on the dielectric strength of BOPP capacitor film. *IEEE Trans Dielectr Electr Insul* 14(5):1295–1301. <https://doi.org/10.1109/TDEI.2007.4339492>
40. Wang L-M (2006) Relationship between intrinsic breakdown field and bandgap of materials. In: 2006 25th International Conference on Microelectronics; IEEE: Belgrade, Serbia and Montenegro, pp 576–579. <https://doi.org/10.1109/ICMEL.2006.1651032>
41. Sun Y, Bealing C, Boggs S, Ramprasad R (2013) 50+ years of intrinsic breakdown. *IEEE Electr Insul Mag* 29(2):8–15. <https://doi.org/10.1109/MEI.2013.6457595>
42. Wang CC, Pilania G, Boggs SA, Kumar S, Breneman C, Ramprasad R (2014) Computational strategies for polymer dielectrics design. *Polymer* 55(4):979–988. <https://doi.org/10.1016/j.polymer.2013.12.069>
43. Sun Y, Boggs S, Ramprasad R (2015) The effect of dipole scattering on intrinsic breakdown strength of polymers. *IEEE Trans Dielectr Electr Insul* 22(1):495–502. <https://doi.org/10.1109/TDEI.2014.004690>
44. Dissado LA, Fothergill JC, Electrical degradation and breakdown in polymers.
45. Chiu F-C (2014) A review on conduction mechanisms in dielectric films. *Adv Mater Sci Eng* 2014:1–18. <https://doi.org/10.1155/2014/578168>
46. Wang J, Guan F, Cui L, Pan J, Wang Q, Zhu L (2014) Achieving high electric energy storage in a polymer nanocomposite at low filling ratios using a highly polarizable phthalocyanine interphase. *J Polym Sci Part B Polym Phys* 52(24):1669–1680. <https://doi.org/10.1002/polb.23554>
47. Wang YU, Tan DQ, Krahn J (2011) Computational study of dielectric composites with core-shell filler particles. *J Appl Phys* 110(4):044103. <https://doi.org/10.1063/1.3624660>
48. Li Q, Zhang G, Liu F, Han K, Gadinski MR, Xiong C, Wang Q (2015) Solution-processed ferroelectric terpolymer nanocomposites with high breakdown strength and energy density utilizing boron nitride nanosheets. *Energy Environ Sci* 8(3):922–931. <https://doi.org/10.1039/C4EE02962C>
49. Alhabill FN, Ayoob R, Andritsch T, Vaughan AS (2018) Introducing particle interphase model for describing the electrical behaviour of nanodielectrics. *Mat Design* 158:62–73. <https://doi.org/10.1016/j.matdes.2018.08.018>

50. Anta JA, Marcelli G, Meunier M, Quirke N (2002) Models of electron trapping and transport in polyethylene: current–voltage characteristics. *J Appl Phys* 92:1002. <https://doi.org/10.1063/1.1489714>
51. Shen Z, Wang J, Lin Y, Nan C, Chen L, Shen Y (2018) High-throughput phase-field design of high-energy-density polymer nanocomposites. *Adv Mater* 30(2):1704380. <https://doi.org/10.1002/adma.201704380>
52. Li Q, Liu F, Yang T, Gadinski MR, Zhang G, Chen L-Q, Wang Q (2016) Sandwich-structured polymer nanocomposites with high energy density and great charge-discharge efficiency at elevated temperatures. *Proc Natl Acad Sci* 113(36):9995–10000. <https://doi.org/10.1073/pnas.1603792113>
53. Andrei L, Ciuprina F (2017) Dielectric properties estimation of nanodielectric interphase by numerical modeling and dielectric spectroscopy. In: 10th International Symposium on Advanced Topics in Electrical Engineering March 23–25. Bucharest, Romania. 519–523. <https://doi.org/10.1109/ATEE.2017.7905100>
54. Qi L, Lee BI, Chen S, Samuels WD, Exarhos GJ (2005) High-dielectric-constant silver-epoxy composites as embedded dielectrics. *Adv Mater* 17(14):1777–1781. <https://doi.org/10.1002/adma.200401816>
55. Xu H-P, Dang Z-M, Jiang M-J, Yao S-H, Bai J (2008) Enhanced dielectric properties and positive temperature coefficient effect in the binary polymer composites with surface modified carbon black. *J Mater Chem* 18(2):229–234. <https://doi.org/10.1039/B713857A>
56. Liu H, Shen Y, Song Y, Nan C-W, Lin Y, Yang X (2011) Carbon nanotube array/polymer core/shell structured composites with high dielectric permittivity, low dielectric loss, and large energy density. *Adv Mater* 23(43):5104–5108. <https://doi.org/10.1002/adma.201102079>
57. Yousefi N, et al (2014) Highly aligned graphene/polymer nanocomposites with excellent dielectric properties for high-performance electromagnetic interference shielding. *Adv Mater* 26(31):5480–5487. <https://doi.org/10.1002/adma.201305293>
58. Chiu B-S, Lin S-T, Duh J-G, Chang P-H (1989) Equivalent circuit model in grain-boundary barrier layer capacitors. *J Am Ceram Soc* 72(10):1967–1975. <https://doi.org/10.1111/j.1151-2916.1989.tb06008.x>
59. Simon P, Gogotsi Y (2008) Materials for electrochemical capacitors. *Nat Mater* 7(11):845–854. <https://doi.org/10.1038/nmat2297>
60. Zhang G, Li Y, Tang S, Thompson RD, Zhu L (2017) The role of field electron emission in polypropylene/aluminum nanodielectrics under high electric fields. *ACS Appl Mater Interfaces* 9(11):10106–10119. <https://doi.org/10.1021/acsami.7b00095>
61. Lu J, Moon K-S, Xu J, Wong CP (2006) Synthesis and dielectric properties of novel high-K polymer composites containing in-situ formed silver nanoparticles for embedded capacitor applications. *J Mater Chem* 16(16):1543. <https://doi.org/10.1039/b514182f>
62. He F, Lau S, Chan HL, Fan J (2009) High dielectric permittivity and low percolation threshold in nanocomposites based on poly(vinylidene fluoride) and exfoliated graphite nanoplates. *Adv Mater* 21(6):710–715. <https://doi.org/10.1002/adma.200801758>
63. Celzard A, McRae E, Furdin G, Maréché JF (1997) Conduction mechanisms in some graphite - polymer composites: the effect of a direct-current electric field. *J Phys Condens Matter* 9(10):2225–2237. <https://doi.org/10.1088/0953-8984/9/10/011>
64. Wu C, Huang X, Wu X, Xie L, Yang K, Jiang P (2013) Graphene oxide-encapsulated carbon nanotube hybrids for high dielectric performance nanocomposites with enhanced energy storage density. *Nanoscale* 5(9):3847. <https://doi.org/10.1039/c3nr00625e>
65. Chen Y et al (2014) Enhanced dielectric properties of amino-modified-CNT/polyimide composite films with a sandwich structure. *J Mater Chem A* 2(34):14118. <https://doi.org/10.1039/C4TA01818D>
66. Zhong S-L et al (2018) Past and future on nanodielectrics. *IET Nanodielect* 1(1):41–47. Accessed 19 Sept 2021. <https://doi.org/10.1049/iet-nde.2018.0004>
67. Chen G, Li ST, Zhong LS (2015) Space charge in nanodielectrics and its impact on electrical performance. In: IEEE 11th International Conference on the Properties and Applications of Dielectric Materials (ICPADM), Sydney, NSW, Australia, July, pp 36–39

68. Zhang L, Khani MM, Krentz TM et al (2017) Suppression of space charge in crosslinked polyethylene filled with poly(stearyl methacrylate)-grafted SiO₂ nanoparticles. *Appl Phys Lett* 110:130903
69. Zhang L, Zhou YX, Tian JH et al (2014) Experiment and simulation of space charge suppression in LDPE/MgO nanocomposite under external DC electric field. *J Electrostat* 72:252–260
70. Wang SJ, Zha JW, Wu YH et al (2015) Preparation, microstructure and properties of polyethylene/alumina nanocomposites for HVDC insulation. *IEEE Trans Dielectr Electr Insul* 22(6):3350–3356
71. Zhou Y, Hu J, Dang B et al (2017) Effect of different nanoparticles on tuning electrical properties of polypropylene nanocomposites. *IEEE Trans Dielectr Electr Insul* 24(3):1380–1413
72. Barber P, Balasubramanian S, Anguchamy Y et al (2009) Polymer composite and nanocomposite dielectric materials for pulse power energy storage. *Materials* 2:1697–1733
73. Dang ZM, Zhou T, Yao SH et al (2009) Advanced calcium copper titanate/polyimide functional hybrid films with high dielectric permittivity. *Adv Mater* 21:2077–2082
74. Dang ZM, Zheng MS, Zha JW (2016) 1D/2D carbon nanomaterial-polymer dielectric composites with high permittivity for power energy storage applications. *Small* 12(13):1–14
75. Yang K, Huang XY, He JL et al (2015) Strawberry-like core-shell Ag@polydopamine@BaTiO₃ hybrid nanoparticles for high-k polymer nanocomposites with high energy density and low dielectric loss. *Adv Mater* 27:1500361
76. Wang YF, Wang LX, Yuan QB et al (2017) Ultrahigh electric displacement and energy density in gradient layer-structured BaTiO₃/PVDF nanocomposites with an interfacial barrier effect. *J. Mater. Chem. A* 5:10849–10855
77. Luo SB, Shen YB, Yu SH et al (2017) Construction of a 3D-BaTiO₃ network leading to significantly enhanced dielectric permittivity and energy storage density of polymer composites. *Energy Environ Sci* 10:137–144
78. Anandraj J, Joshi GM (2017) Fabrication, performance and applications of integrated nanodielectric properties of materials—A review. *Compos Interf*. <https://doi.org/10.1080/09276440.2017.1361717>
79. Chauhan RC, Manmohon S, Baljit S (2007) Rotating machine insulation materials and techniques—an overview. *Indian J Eng Mater Sci* 7:370–374
80. Mitsui H, Yoshida K, Inoue Y et al (1981) Mechanical degradation of high voltage rotating machine insulation. *IEEE Trans Elect Insul EI-16*:351–359
81. Gott BEB, Electr IEEE (1996) *Insul Mag* 12(4):28
82. IEEE Standard 1043 (1989) IEEE recommended practice for voltage-endurance testing of form wound bars and coils
83. Hidinger T, Brockschmidt M, Gröppel P, Weil M, Weidner JR (2016) Improved generator performance with a nanocomposite high voltage insulation system for stator windings—a status report. *GIGRE Paper A1-109*
84. Jiang PK, Chen J, Huang XY (2017) Research status of thermally conductive but electrically insulating polymer nanocomposites (in Chinese). *High Voltage Eng* 43(9):2791–2799
85. Wu K, Li YW, Huang R et al (2017) Constructing conductive multi-walled carbon nanotubes network inside hexagonal boron nitride network in polymer composites for significantly improved dielectric property and thermal conductivity. *Compos Sci Technol* 151:193–201
86. Seyhan AT, Goncu Y, Durukan O et al (2017) Silanization of boron nitride nanosheets (BNNs) through microfluidization and their use for producing thermally conductive and electrically insulating polymer nanocomposites. *J Solid State Chem* 249:98–107
87. Zhang XM, Zhang JJ, Zhang XL et al (2017) Toward high efficiency thermally conductive and electrically insulating pathways through uniformly dispersed and highly oriented graphites close-packed with SiC. *Compos Sci Technol* 150:217–226
88. Sun JJ, Yao YM, Zeng XL et al (2017) Preparation of boron nitride nanosheet/nanofibrillated cellulose nanocomposites with ultrahigh thermal conductivity via engineering interfacial thermal resistance. *Adv Mater Interfaces* 4:1700563
89. Hong HJ, Kwan SM, Lee DS et al (2017) Highly flexible and stretchable thermally conductive composite film by polyurethane supported 3D networks for boron nitride. *Compos Sci Technol* 152:94–100

90. Toohey T, Sottos NR, Lewis JA, Moore JS, White SR (2007) *Nat Mater* 6:581
91. Danikas MD, Tanaka T (2009) Nanocomposites—a review of electrical treeing and breakdown. *IEEE Electr Insul Mag* 25(4):19–25
92. Dissado LA, Mazzanti G, Montanari GC (1997) The role of trapped space charges in the electrical aging of insulating materials. *IEEE Trans Dielectr Electr Insul* 4(5):496–506
93. Krivda A, Tanaka T, Frechette M, Castellon J, Fabiani D, Montanari GC, Gorur R, Morshuis P, Gubanski S, Kindersberger J, Vaughn A, Pelissou S, Tanaka Y, Schmidt LE, Iyer G, Andritsch T, Seiler J, Anglhuber M (2012) Characterization of epoxy microcomposite and nanocomposite materials for power engineering applications. *IEEE Electr. Insul. Mag.* 28(2):38–51
94. Liu L, Zhang C, Luo M et al (2017) A biologically inspired artificial muscle based on fiber-reinforced and electropneumatic dielectric elastomers. *Smart Mater Struct* 26:085018
95. Wang Y, Sun LZ (2017) Development of dielectric elastomer nanocomposites as stretchable actuating materials. *Appl Phys Lett* 111:161904
96. Kwak JW, Chi HJ, Jung KM et al (2005) A face robot actuated with artificial muscle based on dielectric elastomer. *J Mech Sci Technol* 19(2):578–588
97. Chhetry A, Yoon H, Park JY (2017) A flexible and highly sensitive capacitive pressure sensor based on conductive fibers with a microporous dielectric for wearable electronics. *J. Mater. Chem. C* 5:10068–10076
98. Tan DQ (2019) Review of polymer-based nanodielectric exploration and film scale-up for advanced capacitors. *Adv Funct Mat* 30(18):1808567. <https://doi.org/10.1002/adfm.201808567>